

Third-Generation Breathing Metal–Organic Framework with Selective, Stepwise, Reversible, and Hysteretic Adsorption Properties

Suresh Sanda, Srinivasulu Parshamoni, and Sanjit Konar*

Department of Chemistry, IISER Bhopal, Bhopal 462023, India

Supporting Information

ABSTRACT: A new 2D interdigitated and highly flexible, breathing metal–organic framework has been synthesized through a diffusion technique by using the aldrithiol linker and pyromellitate ligand. The compound shows selective, stepwise, reversible, and hysteretic adsorption properties for CO₂ gas and H₂O, MeOH, and CH₃CN vapors.

Metal–organic frameworks (MOFs) are an intriguing class of materials that have attracted intense research attention because of their versatile structural features such as high surface area,^{1a} uniform cavities with predesigned molecular dimensions, and tunable pore size and pore functionalization,^{1b,c} making them very auspicious for a wide range of applications in a variety of areas like gas storage and separation,^{2a} proton conductivity,^{2b} controlled drug delivery, etc.^{2c} An enormous amount of work has been done in this area by scientists like Kitagawa,³ Yaghi,⁴ Férey,⁵ Hupp,⁶ Zhou,⁷ Long,⁸ and several others.⁹ However, one limitation of MOFs is that, once the inorganic nodes are assembled with organic spacers into a crystalline state, they become stationary. In contrast, flexible host frameworks are, in general, guest-responsive, and that is an important criteria for selectivity. Recently, Kitagawa^{10a} and Férey^{10b} reported a few dynamic and flexible so-called third-generation MOFs that show reversible structural changes upon guest adsorption and desorption. Clearfield has also explored some highly robust layered and pillared porous molecules based on phosphonates that show interesting adsorption properties because of either the flexibility of the pillars or their nanosized particles that pack in a “house of cards” arrangement.^{9f} Our effort to develop a guest-responsive flexible framework for selective gas and vapor adsorption resulted in a unique 2D MOF, {[Zn-(C₁₀H₂O₈)_{0.5}(C₁₀S₂N₂H₈)]·5H₂O}_n (**1**), which shows reversible, stepwise, and hysteretic uptake of a large number of gases and vapors.

Compound **1** was synthesized by the reaction of pyromellitate and aldrithiol with Zn(NO₃)₂·6H₂O by a diffusion technique. Single-crystal X-ray diffraction analysis revealed that compound **1** crystallizes in the triclinic *P* $\bar{1}$ space group. The asymmetric unit of **1** contains half of a pyromellitate ligand, one Zn^{II} ion, one aldrithiol linker, and five H₂O molecules. Out of eight oxygen atoms in the pyromellitate ligand, four do not participate in coordination but contribute intermolecular interactions through uncoordinated H₂O molecules. Each Zn^{II} center has four-coordinated tetrahedral geometry, which is fulfilled by two nitrogen atoms from two different aldrithiol ligands and two oxygen atoms from two pyromellitate ligands. Each aldrithiol acts

as a bidentate ligand toward two Zn^{II} ions, whereas each pyromellitate holds four Zn^{II} ions. The opposite carboxylate groups of pyromellitate coordinate to four Zn^{II} ions in a monodentate fashion, forming a 1D chain along the *a* axis; these chains are interconnected by the aldrithiol linkers and give rise to a neutral 2D layered architecture (Figure 1a).

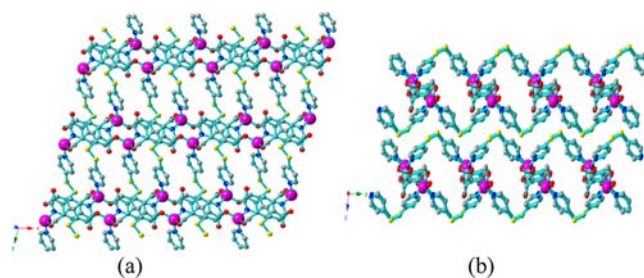


Figure 1. Views of **1** (a) along the *z* axis and (b) along the *x* axis (rhomboidal-shaped 1D channels along the *b* direction). Color code: Zn, magenta; N, blue; C, dark gray; S, yellow; O, red.

Packing of these layers creates rhomboidal-shaped 1D channels with a cross section of $8.6 \times 12.7 \text{ \AA}^2$ that runs along the *b* direction (Figure 1b). The guest H₂O molecules inside the pores are in contact with the free oxygen atoms on the pyromellitate ligand as well as the nearest-neighbor H₂O molecules through hydrogen bonding.

Thermogravimetric analysis (TGA) of compound **1** revealed that the guest H₂O molecules can be completely removed in the temperature range of 100–125 °C with a weight loss of 20%, and the desolvated framework was found to be stable up to 250 °C (Figure S1 in the Supporting Information, SI). The phase purity of the bulk sample was confirmed by powder X-ray diffraction (PXRD; Figure S2 in the SI). The absence of major low-angle peaks in the PXRD pattern (Figure S3 in the SI) of a desolvated sample indicates that the removal of guest molecules causes structural changes in the framework.

Adsorption analysis with N₂ at 77 K shows 3 wt % uptake (Figure 2a), whereas no uptake was observed in the cases of H₂ (77 K) and CH₄ (195 K) (Figure S4 in the SI). If the original cross section of the pores was retained, small molecules like H₂ could have diffused into the pores easily. Interestingly, compound **1** adsorbs a good amount (26.3 wt % at 1 bar) of CO₂ gas at 195 K (Figure 2a). The probable reason behind this selectivity could be the interaction between electron-donating

Received: August 15, 2013

Published: October 30, 2013

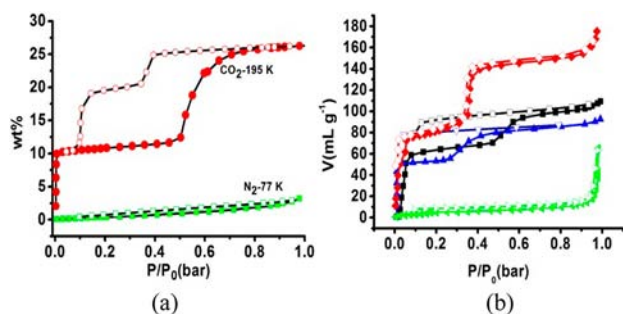


Figure 2. (a) Gas adsorption isotherms at low temperatures: N₂ and 77 K (green); CO₂ and 195 K (red). (b) Solvent sorption isotherms at 298 K: MeOH (red); H₂O (black); CH₃CN (blue); EtOH (green).

uncoordinated oxygen atoms from the pyromellitate ligand and the CO₂ molecule, which results in the enhancement of uptake at low temperature. Zhou et al.¹¹ suggested that CO₂–framework interactions could be strengthened further by the negatively charged groups around the carbon atom. Thallapally et al.^{12a} and Mu et al.^{12b} also suggested that the CO₂ selectivity could be largely enhanced by the formation of an electron donor–acceptor complex because of the incorporation of electron-donating groups into the organic linkers in MOFs. Behind this, we strongly believe that the high quadrupole moment ($-1.4 \times 10^{-39} \text{ Cm}^2$)¹³ of CO₂ might be encouraging the selectivity. The strong interaction between CO₂ and the framework is further confirmed from the isosteric heat of CO₂ adsorption value ($Q_{\text{st}} = -24.21 \text{ kJ mol}^{-1}$ at zero coverage), as calculated from the adsorption data at 273 and 298 K (Figure S5 in the SI). Much less uptake amounts in the cases of H₂ and CH₄ might be due to the weak interaction with the framework, which is also reflected in the isosteric heat of adsorption value ($Q_{\text{st}} = -1.51 \text{ kJ mol}^{-1}$ for H₂ and $Q_{\text{st}} = -16.31 \text{ kJ mol}^{-1}$ for CH₄; Figures S6 and S7 in the SI).

Very surprisingly, we found that, at 195 K, the CO₂ adsorption isotherm exhibits a stepped adsorption curve with two distinct jumps at 0.02 and 0.5 bar. The first step shows a typical type I adsorption isotherm, and the saturation occurs at 0.5 bar with an adsorption amount of 15.8 wt %, whereas the latter step starts from 0.55 bar, with the adsorption amount attaining a value of 26.3 wt % in this case. It is interesting to notice that the desorption curve does not retrace the adsorption pathway and it exhibits two-step desorption at 0.3 and 0.19 bar with a small hysteric-type isotherm with slow kinetics, revealing the strong affinity of the host framework for CO₂. Incomplete desorption indicates that the adsorbed CO₂ is unfavorable to release upon reduction of the external pressure, signifying that it is trapped within the framework. The isotherms at 273 and 298 K (Figure S8 in the SI) show adsorption uptake of 2.5 and 1.2 wt %, respectively, and show no steps in the profile, which indicates that the thermal energy of both the framework and guest molecules reduced their interactions.

To probe and gain more perception into this intriguing sorption behavior, the CO₂ adsorption isotherms were measured at various temperatures in the range of 298–195 K at 1 bar of pressure (Figure S8 in the SI). Notably, above 273 K, the steps in adsorption and desorption are not observed in the entire relative pressure region. So, we anticipate that there is a threshold channel expansion temperature and pressures exists. The increased isosteric heat of adsorption value ($Q_{\text{st}} = -32.76 \text{ kJ mol}^{-1}$), as calculated from the adsorption data at 265 and 273 K (Figure S9 in the SI), further supports that CO₂ is strongly

interacting with the host framework and opens up the channels, which causes the sudden steps in isotherm upon going to the low-temperature region. From the results, we can infer that flexible and dynamic MOFs can exhibit pressure-dependent, stepwise adsorption–desorption isotherms because of a breathing effect, as suggested by Férey et al.,^{14a} Zhou et al.,^{14b} and several others.^{14c,d,6b}

To assess the impression on the structural transformation of the framework, the vapor sorption properties were explored with MeOH, EtOH, CH₃CN, and H₂O at 298 K in its dry form. A quite surprising pathway was observed in the adsorption and desorption profiles of MeOH. The adsorption pathway of MeOH exhibits a three-step adsorption curve (Figure 2b) with three unequivocal jumps at 0.05, 0.3, and 0.9 bar, and the adsorption profile ends up with an adsorption amount of 175 mL g⁻¹. Interestingly, the desorption curve retraces exactly the same pathway. To follow the detailed structural transformation upon adsorption of methanol, we took PXRD patterns of **1** at different vapor-adsorbed states by interrupting the measurement. Careful analysis of the resulting PXRD pattern of step 1 discloses a severe structural change with a shift in the peak positions ($2\theta = 8.5$ and 11.0°) as well as the disappearance of some peaks (such as $2\theta = 12.3^\circ$) and a new peak predominant at $2\theta = 13.2^\circ$ (Figure 3). In

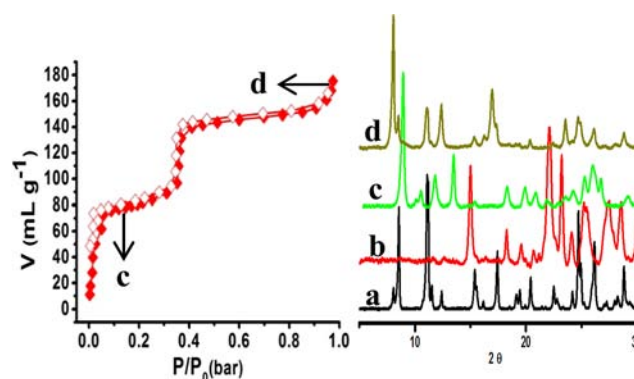


Figure 3. Vapor adsorption isotherm of MeOH (left) and the PXRD patterns (right) of (a) as-synthesized (black) and (b) desolvated (red) compounds (c) at step 1 (green) and (d) after complete adsorption (dark yellow).

the PXRD pattern after complete adsorption steps, the peak at $2\theta = 8.5^\circ$ in the as-synthesized compound was shifted to $2\theta = 8.0^\circ$, revealing that the compound exhibits a structure similar to the as-synthesized one with slight expansion of the framework due to the breathing nature.

The fascinating thing is that the entire structural transformation is reversible with MeOH desorption. Although there are an adequate number of reports explaining the structural transformation, the complete reversible stepwise change along the same path is unprecedented and observed for the first time.

The vapor sorption experiments with CH₃CN and H₂O also show similar adsorption patterns (Figure 2b). In both cases, two-step adsorption isotherms were obtained with a small change in the position of the relative pressure region. The isotherm with CH₃CN showed two noticeable steps at $P/P_0 = 0.03$ and 0.2 bar with a sorption amount of 92.8 mL g⁻¹, whereas H₂O showed 109.5 mL g⁻¹ of uptake with two distinct jumps in the isotherm at $P/P_0 = 0.05$ and 0.4 bar. The sorption isotherm with EtOH displays a sharp single step at 0.9 bar of pressure with an adsorption amount of 65 mL g⁻¹. To affirm the structural transformation, we took PXRD patterns during the experiments

by intruding the measurement after complete adsorption steps (Figure S10 in the SI). The PXRD patterns for CH₃CN and EtOH perfectly matched with the pattern of the MeOH adsorbed sample, indicating that the structure after complete MeOH inclusion is similar to these solvents also. From a comparison of the PXRD patterns at different vapor-adsorbed states to the as-synthesized ones, we concluded that, in the desolvated compound, the peak at (010), which gives information about the interlayer distances (Figure S11 in the SI), was drastically shifted to higher angles, signifying severe shrinkage of the framework due to the removal of guest H₂O molecules, and in the pattern at a complete vapor-adsorbed state, the above-mentioned peak slightly shifted ($2\theta = 0.5^\circ$) to lower angles, confirming the slight expansion of the framework and also reflecting the breathing mechanism in the presence of solvent vapors.

The PXRD pattern of H₂O is exactly similar to that of the as-synthesized compound. This is unsurprising because compound **1** achieved its original structure as a result of reaccumulation of H₂O molecules inside the pores, and the strong hydrogen-bonding interactions between uncoordinated carboxylate oxygen atoms and free H₂O molecules restrict the framework from expanding. The single step as well as smaller adsorption amount in the case of EtOH can be justified by correlating the large molecular diameter (4.3 Å) and less polarity of EtOH compared to other solvents, whereas the noticeable steps in the case of CH₃CN and H₂O could be ascribed by considering the relatively small kinetic diameter (4.0 Å) compared to EtOH.

In conclusion, we report the synthesis and characterization of a breathing MOF, which shows reversible and stepwise adsorption toward a large number of adsorbates like CO₂ gas and MeOH, H₂O, and CH₃CN vapors. The results push the boundary in the area of “soft-MOF” for designing a global molecular sponge. Two-step adsorption indicates unusual structural changes in the framework due to a “breathing effect”. Although several MOFs show a structural change by external stimuli, only a few show a definite stepwise sorption isotherm related to a “breathing effect”,^{10b,14b} and there is no report of any MOF that shows stepwise, reversible, and hysteretic adsorption toward more than one adsorbate. The first step of adsorption can be accounted for through filling of the 1D channels, and the second step could be due to filling of the 2D interlayer spacing between the layers.¹⁵ However, detailed further studies are needed to come to an unambiguous conclusion.

■ ASSOCIATED CONTENT

■ Supporting Information

X-ray crystallographic data in CIF format, details of the synthesis for compound **1**, PXRD patterns at different conditions, gas sorption isotherms, TGA, IR data, and additional figures. This material is available free of charge via the Internet at <http://pubs.acs.org>.

■ AUTHOR INFORMATION

Corresponding Author

*E-mail: skonar@iiserb.ac.in.

Notes

The authors declare no competing financial interest.

■ ACKNOWLEDGMENTS

S.S. and S.P. thank IISER Bhopal for Ph.D. fellowships. S.K. thanks CSIR, Government of India [Project 01/(2473)/11/

EMRII], and IISER Bhopal for generous financial and infra-structural support.

■ REFERENCES

- (1) (a) Farha, O. K.; Eryazici, I.; Jeong, N. C.; Hauser, B. G.; Wilmer, C. E.; Sarjeant, A. A.; Snurr, R. Q.; Nguyen, S. T.; Yazaydin, A. O.; Hupp, J. T. *J. Am. Chem. Soc.* **2012**, *134*, 15016–15021. (b) Uemura, T.; Yanaia, N.; Kitagawa, S. *Chem. Soc. Rev.* **2009**, *38*, 1228–1236. (c) Kepert, C. J. *Chem. Commun.* **2006**, 695–700.
- (2) (a) Li, J. R.; Sculley, J.; Zhou, H. C. *Chem. Rev.* **2012**, *112*, 869–932. (b) Hurd, J. A.; Vaidhyanathan, R.; Thangadurai, V.; Ratcliffe, C. L.; Moudrakovski, I. L.; Shimizu, G. K. H. *Nat. Chem.* **2009**, *1*, 705–710. (c) Rocca, J. D.; Liu, D.; Lin, W. *Acc. Chem. Res.* **2011**, *44*, 957–968.
- (3) (a) Sakata, Y.; Furukawa, S.; Kondo, M.; Hirai, K.; Horike, N.; Takashima, Y.; Uehara, H.; Louvain, N.; Meilikhov, M.; Tsuruoka, T.; Isoda, S.; Kosaka, W.; Sakata, O.; Kitagawa, S. *Science* **2013**, *339*, 193–196. (b) Uemura, K.; Kitagawa, S. *Chem. Soc. Rev.* **2005**, *34*, 109–119.
- (4) (a) Ockwig, N.; Friedrichs, O.; O’Keeffe, M.; Yaghi, O. M. *Acc. Chem. Res.* **2005**, *38*, 176–182. (b) Deng, H.; Grunder, S.; Cordova, K. E.; Valente, C.; Furukawa, H.; Hmadeh, M.; Gandara, F.; Whalley, A. C.; Liu, Z.; Asahina, S.; Kazumori, H.; O’Keeffe, M.; Terasaki, O.; Stoddart, J. F.; Yaghi, O. M. *Science* **2012**, *336*, 1018–1023.
- (5) (a) Férey, G. *Chem. Soc. Rev.* **2008**, *37*, 191–214. (b) Draznieks, C. M.; Serre, C.; Millange, F.; Férey, G. *Acc. Chem. Res.* **2005**, *38*, 217–225.
- (6) (a) Jeong, N. C.; Samanta, B.; Lee, C. Y.; Farha, O. K.; Hupp, J. T. *J. Am. Chem. Soc.* **2012**, *134*, 51–54. (b) Mulfort, K. L.; Farha, O. K.; Malliakas, C. D.; Kanatzidis, M. G.; Hupp, J. T. *Chem.—Eur. J.* **2010**, *16*, 276–281. (c) Farha, O. K.; Hupp, J. T. *Acc. Chem. Res.* **2010**, *43*, 1166–1175.
- (7) (a) Park, J.; Yuan, D.; Pham, K. T.; Li, J. R.; Yakovenko, A.; Zhou, H. C. *J. Am. Chem. Soc.* **2012**, *134*, 99–102. (b) Li, J. R.; Zhou, H. C. *Nat. Chem.* **2010**, *2*, 893–898. (c) Zhao, D.; Timmons, D. J.; Yuan, D.; Zhou, H. C. *Acc. Chem. Res.* **2011**, *44*, 123–133.
- (8) (a) Herm, Z. R.; Wiers, B. M.; Mason, J. A.; van Baten, J. M.; Hudson, M. R.; Zajdel, P.; Brown, C. M.; Masciocchi, N.; Krishna, R.; Long, J. R. *Science* **2013**, *340*, 960–964. (b) Sumida, K.; Rogow, D. L.; Mason, J. A.; McDonald, T. M.; Bloch, E. D.; Herm, Z. R.; Bae, T. H.; Long, J. R. *Chem. Rev.* **2012**, *112*, 724–781 and references cited therein.
- (9) (a) Chapman, K. W.; Halder, G. J.; Chupas, P. J. *J. Am. Chem. Soc.* **2009**, *131*, 17546–17547. (b) Plonka, A. M.; Banerjee, D.; Woerner, W. R.; Zhang, Z.; Nijem, N.; Chabal, Y. J.; Li, J.; Parise, J. B. *Angew. Chem., Int. Ed.* **2013**, *52*, 1692–1695. (c) Ma, L.; Abney, C.; Lin, W. *Chem. Soc. Rev.* **2009**, *38*, 1248–1256 and references cited therein. (d) Chen, B.; Xiang, S.; Qian, G. *Acc. Chem. Res.* **2010**, *43*, 1115–1124. (e) Wang, Z. Q.; Cohen, S. M. *Chem. Soc. Rev.* **2009**, *38*, 1315–1329. (f) Clearfield, A. *Dalton Trans.* **2008**, 6089–6102.
- (10) (a) Seo, J.; Matsuda, R.; Sakamoto, H.; Bonneau, C.; Kitagawa, S. *J. Am. Chem. Soc.* **2009**, *131*, 12792–12800. (b) Beurroies, I.; Boulhout, M.; Llewellyn, P. L.; Kuchta, B.; Férey, G.; Serre, C.; Denoyel, R. *Angew. Chem., Int. Ed.* **2010**, *49*, 7526–7529.
- (11) Li, J. R.; Yu, J.; Lu, W.; Sun, L. B.; Sculley, J.; Balbuena, P. B.; Zhou, H. C. *Nat. Commun.* **2013**, *4*, 1538, DOI: 10.1038/ncomms2552.
- (12) (a) Liu, J.; Thallapally, P. K.; McGrail, B. P.; Brown, D. R.; Liu, J. *Chem. Soc. Rev.* **2012**, *41*, 2308–2322. (b) Mu, W.; Liu, D. H.; Yang, Q. Y.; Zhong, C. L. *Microporous Mesoporous Mater.* **2010**, *130*, 76–82.
- (13) (a) Bae, Y. S.; Farha, O. K.; Spokoyny, A. M.; Mirkin, C. A.; Hupp, J. T.; Snurr, R. Q. *Chem. Commun.* **2008**, 4135–4137. (b) Choi, H. S.; Suh, M. P. *Angew. Chem., Int. Ed.* **2009**, *48*, 6865–6869.
- (14) (a) Ramsahye, N. A.; Maurin, G.; Bourrelly, S.; Llewellyn, P. L.; Loiseau, T.; Serre, C.; Férey, G. *Chem. Commun.* **2007**, 3261–3263. (b) Yuan, D.; Getman, R. B.; Wei, Z.; Snurr, R. Q.; Zhou, H. C. *Chem. Commun.* **2012**, *48*, 3297–3299. (c) Nijem, N.; Wu, H.; Canepa, P.; Marti, A.; Balkus, K. J.; Thonhauser, T., Jr.; Li, J.; Chabal, Y. J. *J. Am. Chem. Soc.* **2012**, *134*, 15201–15204. (d) Choi, H. J.; Dinca, M.; Long, J. R. *J. Am. Chem. Soc.* **2008**, *130*, 7848–7850.
- (15) Kanoo, P.; Mostafa, G.; Matsuda, R.; Kitagawa, S.; Maji, T. K. *Chem. Commun.* **2011**, *47*, 8106–8108.